

Synthesis and characterization of structural and magnetic properties of Fe doped NiO nanoparticles

M. Venkatachalapathy^a, K. Sambathkumar^{b,*}, N. R. Kamal^a

^aPG& Research Department of Physics Thiru. A. Govindasamy Government Arts CollegeTindivanam, Tamil Nādu, 604 307, India.

^bPG& Research Department of Physics Arraigner Anna Government Arts College, Villupuram, Tamil Nādu, 605 602, India.

The innovative nanocrystalline pure and Fe doped NiO nanoparticles have been prepared successfully by a chemical method. NiO and Fe doped NiO nanoparticles have been characterized using various analytical techniques such as ultraviolet-visible spectrometer [UV-Vis] absorption in florescence emission spectroscopy. Ray diffraction [XRD] Fourier transform infrared spectroscopy [FTIR], scanning electron microscope [SEM] The average grain size of NiO nano articles and Fe doped NiO nanoparticles are respectively. The UV absorbance fig shows a strong absorption peak present 310nm. The band gap values of NiO nanoparticles and Fe doped NiO nanoparticles are 3.37eV and 3.7eV. The assimilation of Fe into NiO nanoparticles have strongly influenced the magnetic behaviour and the material got converted from ferromagnetic to anti ferromagnetic material.

(Received November 8, 2023; Accepted March 26, 2024)

Keywords: Nickel oxide, Elemental quantitative information, X-ray diffraction, VSM

1. Introduction

The antiferromagnetic (AF) metal oxide nanoparticles (NPs) have attracted enormous attention because of their hopeful technological applications and essential physics. The effect of finite size leads to the accumulation of frustrating surface spins and various point defects at the surface of the AF NPs, which results in an intersisting magnetic and optical properties that differ significantly from their bulk counterparts [1], Among the various AF Materials, nickel oxide (NiO) is one of the few P-type semiconductors (acceptor state induced by the nickel vacancy (V_{Ni}) with a wide -bandgap E.g., =4eV) having face -centered-cubic(fcc) crystal symmetry. In the bulk form, NiO possesses AF ordering with the Neel transition temperature 523K [2]. However, NiO nanostructure exhibits anomalous magnetic properties that are very sensitive to size, Ni vacancy defects, morphology, and crystal structure, thus showing a wide variety of intriguing phenomena. It has been reported that below a particle size of $d=0nm$, the long -rang ordered $Ni^{2+}O_2-Ni^{2+}$ super exchange interaction breakdown, due to an enhanced V_{Ni} defect resulting in a weak ferromagnetic (FM) like properties [.3,4], Furthermore, the effect of frustrating surface spins become more dominant below $d=10nm$ [5,6,7]. The NiO nanostructures have been used in rechargeable batteries [8], magnetic recording media [9], the next -generation resistive switching memory devices [10], and so on. Recently, functionalized NiO nanostructures have attracted great research interest from both fundamental and application point of view [11,12], the further development in functionalized NiO nanostructure is focused on obtaining a room temperature (RT) ferromagnetism without comparing the structure in order to facilitate the possible integration of spintronic devices.

According to recent findings, RT ferromagnetism in NiO NPs can be achieved through transition metal(TM)-doping , for example ,Fe (either due to substitution or the formed defect clusters), which opens up their potential applications in the future advanced spintronic devices[13-15].The properties of such a system can be tailored by controlling both the particle size and Fe-dopant concentration ,which results in a complex magnetic property[16-22].For instance, the

*Corresponding author: sambathdft@gmail.com

<https://doi.org/10.15251/DJNB.2024.191.451>

doping of Fe⁺ ions can alter the Ni²⁺-O₂-Fe³⁺ super exchange interaction and so the AF properties. Whereas ions at the interstitial site could form 4:1 defect cluster consisting of tetravalent interstitial whereas, Fe ions at the interstitial site could form 4:1 defect cluster consisting of tetravalent interstitial and four VNi, in total being four times negatively charged [16,23-27]. Such a complex structure could result in interesting magnetic properties. According to previous reports, bare and Fe-doped NiO NPs both exhibit low-temperature magnetic memory effect [16,28,29]. Such a type of nanoscale system can be used as a "thermal assistant memory cell" in digital information storage [31,32]. However, the magnetic memory effect is mostly observed in the low-temperature region far below the RT, and this is the major obstacle precluding its application in nanotechnology. The above obstacle has been foiled through introducing exchange-coupling [30,33] and particle size distribution [34]. In this study we have reported RT magnetic memory effect from Fe-doped NiO NPs synthesized using a chemical method followed by thermal treatment in the air. Thorough investigation of structure and four VNi, in total being four times negatively charged [16,23-27]. Such a complex structure could result in interesting magnetic properties. According to previous reports, bare and the Fe-doped NiO NPs both exhibit low-temperature magnetic memory effect [16,28,29]. Such a type of nanoscale system can be used as a "thermal assistant memory cell" in digital information storage [30-32]. However, the magnetic memory effect is mostly observed in the low-temperature region far below the RT, and this is the major obstacle precluding its application in nanotechnology. In the past, the above obstacle has been foiled through introducing exchange-coupling [30,33] and particle size distribution [34]. In this study, we have reported RT magnetic memory effect from Fe-doped NiO NPs synthesized using a co-precipitation method followed by thermal treatment in the air. A thorough investigation of structural and magnetic properties was carried out using synchrotron radiation powder X-ray diffraction (PXRD), neutron powder diffraction (NPD), and dc magnetometer. Our findings suggest that the RT magnetic memory effect in Fe-doped NiO NPs is mediated through intrinsic intraparticle interactions. And magnetic properties were carried out using synchrotron radiation powder X-ray diffraction [PXRD], neutron powder diffraction [NPD], and dc magnetometer. Our findings suggest that the RT magnetic memory effect in Fe-doped NiO NPs is mediated through intrinsic intraparticle interactions.

2. Experimental details

2.1. Synthesis method and material

All of the analytical grade In the starting Nickel II acetate tetrahydrate [(CH₃COO)₂NiO.4H₂O] taken around 13grams dissolved in the 50 ml water and stirred using Magnetic stirrer up to 3hours. After aqueous of 6 grams NaOH is added drop wise to the above mixture so that solution was added in the green color light due to stirrer will up to 3hours the Perfectly mixed solution another dopant Iron (II)acetate Tetrahydrate [(CH₃COO)₂Fe.4H₂O] solution I will take separate magnetic stirrer in 3 hours after in the solution a beaker drop wise to drop wise the first main solution added the solution stirred up to 24 hours then the fully saturated the solution filtered with Mann papers and the precipitated compound mixed ethanol this process called purification four time. The ethanol mixed precipitated solution subjected to micro-hot air Oven at range of 130-degree temperature during 48 hours due to this process the color of sample little changed instead of light green. The wet sample again maintained at muffle furnace in order to 550-degree temperature using crucible. Finally received the highly melted little grain sized samples to transfer powder form by agate mortar. Thus, the Fe doped NiO nano powder harvested with ash color and carried out to some characterization and magnetic studies.

3. Results and characterization

3.1. X-ray diffraction studies

The diffraction patterns of the as synthesized nickel acetate nanoparticles obtained respectively, show sharp and intense peaks which clearly indicate that the particles are crystalline. Representative X-ray diffraction pattern is presented in Fig. The XRD patterns of the Pure NiO and Fe doped NiO nanoparticles showed diffraction peaks absorbed at 2θ values (Fig.1). The average crystallite size (D) of nanoparticles was calculated using the Scherrer formula as follows:

$$D_{h,k,l} = (0.9\lambda / \beta_{h,k,l} \cos\theta) \quad (1)$$

where λ is the wavelength ($\lambda = 1.542 \text{ \AA}$) ($\text{CuK}\alpha$), β is the full width at half maximum (FWHM) of the line, and θ is the diffraction angle. All the diffraction peaks can be indexed to the face-centered cubic structure of NiO (JCPDS # 47-1049 with a* quality) with lattice parameters $a = 4.1771 \text{ \AA}$. It is obvious from the figure, that the all samples had same diffraction peaks and are indexed as phase with XRD pattern 002, 111, 200, 111, 202, and 220 comparable with the JCPDS. No other peaks were observed, indicating that the $\text{NiCO}_3 \cdot 2\text{Ni(OH)}_2 \cdot x\text{H}_2\text{O}$ was completely decomposed to NiO after the calcination. The average crystallite sizes calculated by applying the Scherrer formula to the diffraction peaks are 13.92 nm at 300 °C.

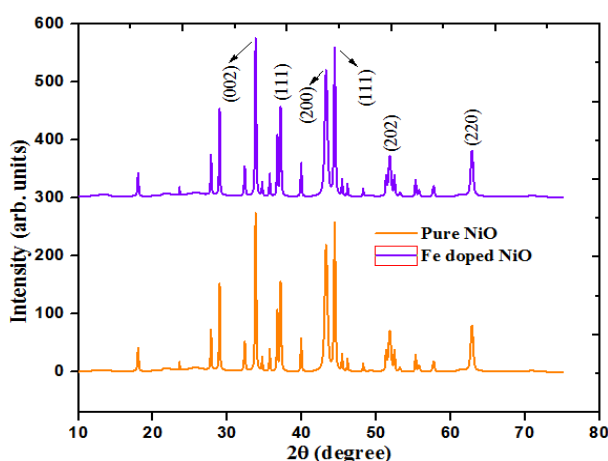


Fig.1. The XRD Pattern of Pure NiO and Fe doped NiO nanoparticles.

3.2. UV analysis

The optical absorption spectra of Fe doped NiO NPs are shown in Fig. Absorption maximum of NiO is 250 nm (3.9 eV) and that of NiO is 285 nm (3.37 eV) as observed in Fig. An additional peak at 310 nm (3.6 eV) is also observed for Fe doped NiO.

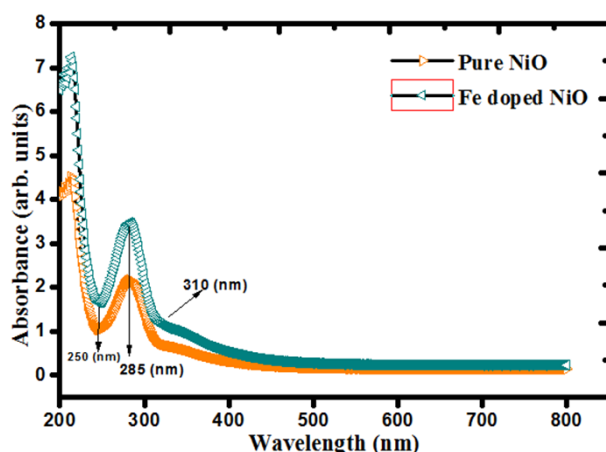


Fig.2. UV-vis Spectrum of Pure NiO and Fe doped NiO nanoparticles.

The presence of this additional peak has also been reported by Qi et al., [35] and Sri- Vat Sava and Srivastava [36]. This blue shift of the absorption edges for different sized nanocrystals is related to the size decrease of particles due to the quantum confinement effect of nanoparticles. It is necessary to mention that the optical direct band gap values of the NiO samples were determined by Talc's relation [37]

$$\alpha h\nu = \alpha_0 (h\nu - E_g)^{1/2}$$

where $h\nu$, α_0 and E_g , are photon energy, a constant and optical band gap of the nanoparticles, respectively. Absorption coefficient (α) of the powders at different wavelengths can be calculated from the absorption spectra. The values of E_g , were determined by extrapolations of the linear regions of the plot of $(\alpha h\nu)^2$ versus $h\nu$. We calculate the size of the nanoparticles.

3.3. FTIR analysis

Pure and Fe doped NiO shows FT-IR transmission spectra were taken on JASCO 640 plus infrared spectrometer in the range of 4000–400 cm^{-1} at room temp. Samples were prepared by mixing samples powder with KBr, which were ground and pressed into a transparent pellet with a diameter of cm^{-1} . The peak around 3400 cm^{-1} on the FT-IR spectrum is related to O-H bond. The absorption at 1110 cm^{-1} attributed to hydroxyl groups. The absorption bonds at 1420 cm^{-1} and 1110 cm^{-1} indicates the existence of carbonates and the bond at 3400 cm^{-1} correspond to C-H stretching mode [38] As shown in fig, The absorption bonds at 870 and 600 cm^{-1} are associated to Ni-O vibration bond, but absorption bond at 619 cm^{-1} is assigned to Ni-O-H stretching bond. The above information confirmed formation of pure NiO nanoparticle. Presence of Carbon impurity in the samples is because of ethanol, which is used for washing. As shown in fig, the absorption bonds at 447 cm^{-1} are associated to Ni-O vibration bond [39] but absorption bond at 600 cm^{-1} is assigned to Ni- O-H stretching bond. FTIR spectrum of the Fe doped NiO nanoparticle before Calcination at room temp.

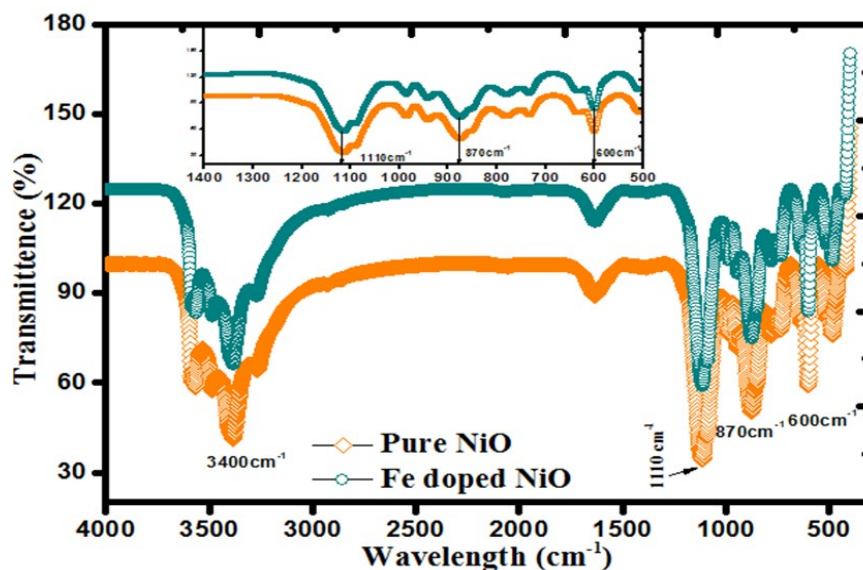


Fig.3. FTIR Spectrum of Pure NiO and Fe doped NiO nanoparticles.

3.4. SEM with EDX

Shows the different morphologies of the as-synthesized NiO nanoparticles using different doped. The SEM images clearly show nano-structural homogeneities and remarkably different morphologies for the as-synthesized Fe doped NiO nanoparticles. The shapes of the as-synthesized Fe doped NiO nanoparticles of the methanol and ethanol mediated samples are shown in Fig; an agglomeration of nanoparticles was observed in most of the cases. These images show the cauliflower-petal like morphologies, which consists of spherical and elliptical shape of NiO nanoparticles. Sheet- or snowflake-like morphology was observed for the water mediated sample, The nanoparticles size calculated in the SEM images was approximately in good agreement with the particle size calculated from the XRD analysis. The pure and Fe doped NiO nanoparticles size and morphology reveals the key role of the individual solvents in controlling the nucleation and crystal orientation [40]. The average size of the NiO nanoparticle observed from SEM images is 24 nm. Crystallinity is evaluated through comparison of crystallite size as ascertained by SEM particle size determination. The resultant solution for pure NiO and Fe doped NiO samples was examined utilizing energy dispersive X-ray analysis, as seen in Fig. NiO nanoparticles were analyzed by EDX at 10 keV. The existence of Nickel (Ni) and oxygen (O) elements was discovered in NiO NPs, with results suggested that the nanoparticles remained almost stoichiometric. The mass percentage of nickel and oxide determined from EDX examination were Ni 96.43 wt.% percent (0.804 keV) and O 3.57 wt.% percent (0.804 keV), correspondingly, and no additional elemental impurities were found as pure EDX spectrum. From Fig. Fe doped NiO NPs occurrence of Nickel (Ni), oxygen (O) and Iron (Fe) elements in NiO NPs. The Fe doped NiO indicates the weight % is calculated from EDX analysis was (Fe) 1.1 wt.% (0.4 keV). This finding validated the synthesis of pure NiO nanoparticles.

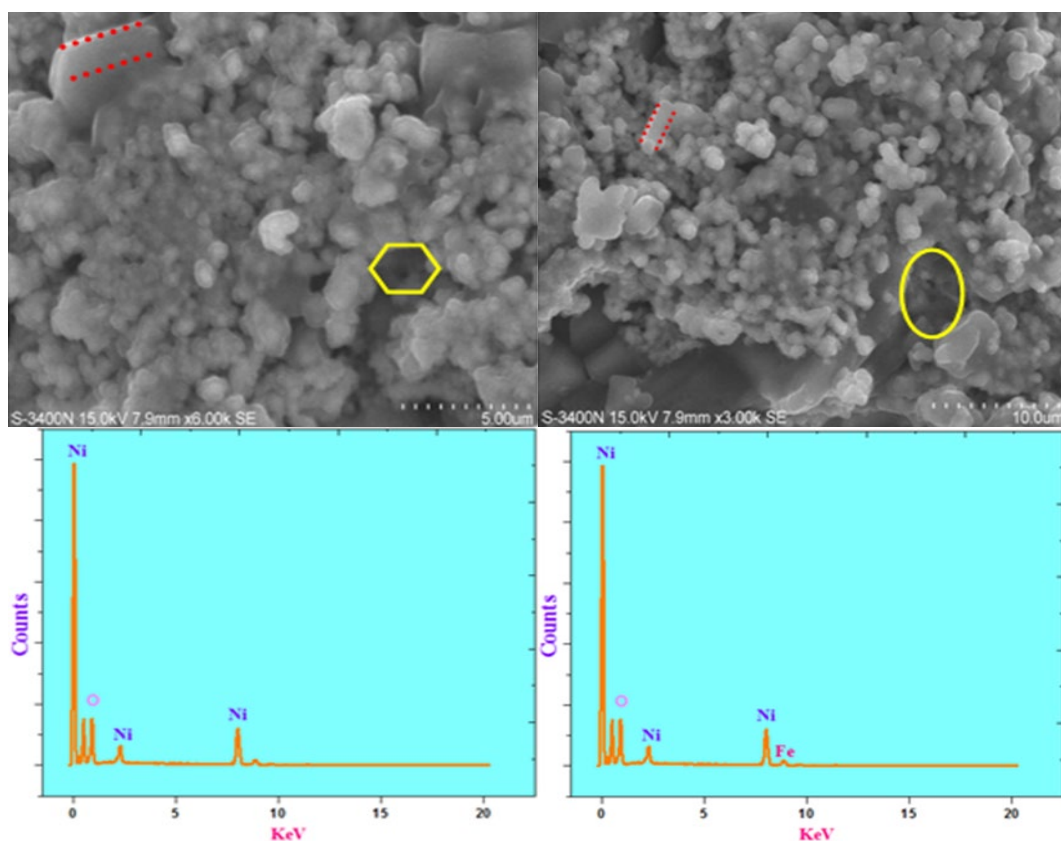


Fig.4. SEM with EDX pure NiO and Fe doped NiONps.

3.5. Vibrating Sample Magnetometer (VSM)

Magnetization measurements of NiO nanoparticles were performed using VSM technique at fields of -15000 to 15000 Oersted at room temperature are shown in Fig.5 before and after doping, respectively. VSMs were used in this study, which used an applied magnetic field of 10 kOe while operating at room temperature (RT). These results help to analyse the effects of saturation magnetization, coercive and residual magnetization, and M- H hysteresis loops have all been studied in the context of NiO nanomaterials. It is seen that the NiO nanoparticles exhibit superparamagnetic behaviour at room temperature. VSM results exhibit well-defined S-shaped curve as response of the sample against applied magnetic field. As an effect of additive incorporations, the saturation magnetization and the coercive field strength show a decreasing trend with increasing Fe concentration in NiO nanostructure. The remanent magnetizations almost decrease with increasing 'Fe' concentration in NiO nanomaterial. It is because of the stretch at the grid point. It has been reported elsewhere [41,42], coercive effect of pure NiO and additive incorporated NiO is influenced greatly by factors such as anisotropy, particle morphology, porosity, micro-expansion, size distribution, and the size of the magnetic domain are all characteristics that may be measured. It has been observed that Fe is an element with soft magnetic characteristics, by nature, and this soft nature is speculated to be lost while incorporating with NiO.

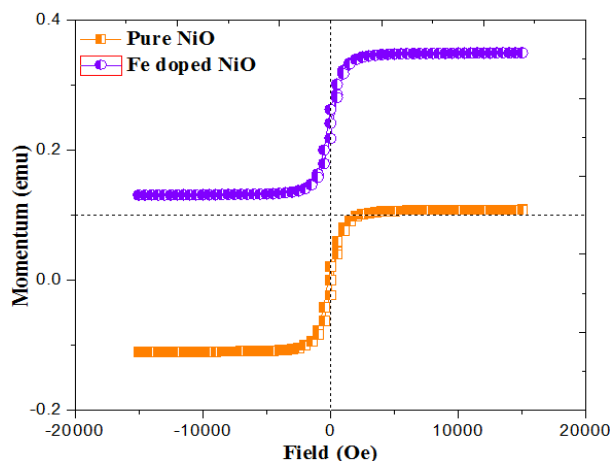


Fig.5. VSM Analyser of Pure NiO and Fe doped NiO nanoparticles.

4. Conclusion

In Fe doped NiO powder prepared by co-precipitation from acetate precursors, we show that the size of crystallites metrically decreases with increasing Fe concentration. The XRD patterns of the nanoparticles showed that correspond to face centered cubic structure of Fe doped NiO nano particles. The particles are larger than the threshold value below which finite size effect dominates. The observed magnetic behavior therefore is a consequence of Fe induced magnetic ordering in the bulk of NiO. In addition, some amount of magnetic in homogeneity also contributes to the magnetic characteristics of Fe doped NiO as evidenced from the temperature dependent magnetization study under field cooled and zero field cooled conditions. The optical absorption spectra of Fe doped NiO NPs are shown in Fig. Absorption maximum of NiO is 250 nm (3.9 eV) and that of NiO is 285 nm (3.37 eV) as observed. An additional peak at 310 nm (3.6 eV) is also observed for Fe doped NiO. The absorption bonds at 870 and 600 cm^{-1} are associated to Ni-O vibration bond, but absorption bond at 619 cm^{-1} is assigned to Ni-O-H stretching bond. The above information confirmed formation of pure NiO nanoparticle. The SEM images clearly show nano-structural homogeneities and remarkably different morphologies for the as-synthesized Fe doped NiO nanoparticles. The Fe doped NiO indicates the weight % is calculated from EDX analysis. VSM results exhibit well-defined S-shaped curve as response of the sample against applied magnetic field.

References

- [1] Kodama, R.H.; Makhlof, S.A.; Berkowitz, A.E., Phys. Rev. Lett. 1997, 79, 1393-1396; <https://doi.org/10.1103/PhysRevLett.79.1393>
- [2] Gandhi, A.C.; Wu, S.Y., Nanomaterials 2017, 7, 231; <https://doi.org/10.3390/nano7080231>
- [3] Gandhi, A.C.; Pant, J.; Wu, S.Y., RSC Adv. 2016, 6, 2079-2086; <https://doi.org/10.1039/C5RA24673C>
- [4] Mandal, S.; Banerjee, S.; Menon, K.S.R., Phys. Rev. B 2009, 80, 214420; <https://doi.org/10.1103/PhysRevB.80.214420>
- [5] Gandhi, A.C.; Pant, J.; Pandit, S.D.; Dalimbkar, S.K.; Chan, T.S.; Cheng, C.L.; Ma, Y.R.; Wu, S.Y., J. Phys. Chem. C 2013, 117, 18666-18674; <https://doi.org/10.1021/jp4029479>
- [6] Rinaldi-Montes, N.; Gorria, P.; Martínez-Blanco, D.; Fuertes, A.B.; FernándezBarquín, L.; Rodríguez Fernández, J.; de Pedro, I.; Fdez-Gubieda, M.L.; Alonso, J.; Olivi, L.; et al., Nanoscale 2014, 6, 457-465; <https://doi.org/10.1039/C3NR03961G>
- [7] Tiwari, S.D.; Rajeev, K.P., Phys. Rev. B 2005, 72, 104433;

<https://doi.org/10.1103/PhysRevB.72.104433>

- [8] Lee, D.U.; Fu, J.; Park, M.G.; Liu, H.; Kashkooli, A.G.; Chen, Z., *Nano Lett.* 2016, 16, 1794-1802; <https://doi.org/10.1021/acs.nanolett.5b04788>
- [9] Rinaldi-Montes, N.; Gorria, P.; Martínez-Blanco, D.; Fuertes, A.B.; Puente-Orench, I.; Olivi, L.; Blanco, J.A., *AIP Adv.* 2016, 6, 056104; <https://doi.org/10.1063/1.4943062>
- [10] Oka, K.; Yanagida, T.; Nagashima, K.; Kawai, T.; Kim, J.S.; Park, B.H., *J. Am. Chem. Soc.* 2010, 132, 6634-6635; <https://doi.org/10.1021/ja101742f>
- [11] Sasaki, T.; Devred, F.; Eloy, P.; Gaigneaux, E.M.; Hara, T.; Shimazu, S.; Ichikuni, N., *Bull. Chem. Soc. Jpn.* 2009, 92, 840-846; <https://doi.org/10.1246/bcsj.20180387>
- [12] Ouyang, Y.; Huang, R.; Xia, X.; Ye, H.; Jiao, X.; Wang, L.; Lei, W.; Hao, Q., *Chem. Eng.* 2018, 355, 416-427; <https://doi.org/10.1016/j.cej.2018.08.142>
- [13] Wang, J.; Cai, J.; Lin, Y.-H.; Nan, C.-W., *Appl. Phys. Lett.* 2005, 87, 202501; <https://doi.org/10.1063/1.2130532>
- [14] Shim, J.H.; Hwang, T.; Lee, S.; Park, J.H.; Han, S.J.; Jeong, Y.H., *Appl. Phys. Lett.* 2005, 86, 082503; <https://doi.org/10.1063/1.1868872>
- [15] Lee, H.-J.; Jeong, S.-Y.; Cho, C.R.; Park, C.H., *Appl. Phys. Lett.* 2002, 81, 4020-4022; <https://doi.org/10.1063/1.1517405>
- [16] Gandhi, A.C.; Pradeep, R.; Yeh, Y.C.; Li, T.Y.; Wang, C.Y.; Hayakawa, Y.; Wu, S.Y., *ACS Appl. Nano Mater.* 2019, 2, 278-290; <https://doi.org/10.1021/acsanm.8b01898>
- [17] Moura, K.O.; Lima, R.J.S.; Coelho, A.A.; Souza-Junior, E.A.; Duque, J.G.S.; Meneses, C.T., *Nanoscale* 2014, 6, 352-357; <https://doi.org/10.1039/C3NR04926D>
- [18] Kurokawa, A.; Sakai, N.; Zhu, L.; Takeuchi, H.; Yano, S.; Yanoh, T.; Onuma, K.; Kondo, T.; Miike, K.; Miyasaka, T.; et al., *J. Korean Phys. Soc.* 2013, 63, 716; <https://doi.org/10.3938/jkps.63.716>
- [19] Mishra, A.K.; Bandyopadhyay, S.; Das, D., *Mater. Res. Bull.* 2012, 47, 2288-2293; <https://doi.org/10.1016/j.materresbull.2012.05.046>
- [21] Manna, S.; Deb, A.K.; Jagannath, J.; De, S.K., *J. Phys. Chem. C* 2008, 112, 10659-10662; <https://doi.org/10.1021/jp711943m>
- [22] He, J.H.; Yuan, S.L.; Yin, Y.S.; Tian, Z.M.; Li, P.; Wang, Y.Q.; Liu, K.L.; Wang, C.H., *J. Appl. Phys.* 2008, 103, 023906; <https://doi.org/10.1063/1.2832437>
- [23] M. Chandrasekar, M. Subash, S. Logambal, G. Udhayakumar, R. Uthrakumar, C. Inmozhi, Wedad A. Al-Onazi, Amal M. Al-Mohaimed, Tse-Wei Chen, K. Kanimozhi, *Journal of King Saud University - Science*. Volume: 34 (2022) 101831; <https://doi.org/10.1016/j.jksus.2022.101831>
- [24] Krafft, K.N.; Martin, M. A., *Korean J. Ceram.* 1998, 4, 156-161. [Google Scholar]
- [25] Hoser, A.; Martin, M.; Schweika, W.; Carlsson, A.E.; Caudron, R.; Pyka, N., *Solid State Ion.* 1994, 72, 72-75; [https://doi.org/10.1016/0167-2738\(94\)90127-9](https://doi.org/10.1016/0167-2738(94)90127-9)
- [26] M. Venkatachalapathy, N. Rajkamal, K. Sambathkumar, *Digest Journal of Nanomaterials and Biostructures* Vol. 17, No. 4, October-December 2022, 1441-1451; <https://doi.org/10.15251/DJNB.2022.174.1441>
- [27] Haaß, F.; Buhrmester, T.; Martin, M., *Phys. Chem. Chem. Phys.* 2001, 3, 4806-4810; <https://doi.org/10.1039/b103884m>
- [28] Gandhi, A.C.; Chan, T.S.; Pant, J.; Wu, S.Y., *Nanoscale Res. Lett.* 2017, 12, 1-8; <https://doi.org/10.1186/s11671-017-1988-x>
- [29] M. Chandrasekar, S. Panimalar, R. Uthrakumar, M. Kumar, M.E. Raja Saravanan, G. Gobi, P. Matheswaran, C. Inmozhi, K. Kaviyarasu, *Materials Today: Proceedings*. Volume: 36 (2021) 228-231; <https://doi.org/10.1016/j.matpr.2020.03.228>
- [30] Xu, L.; Gao, Y.; Malik, A.; Liu, Y.; Gong, G.; Wang, Y.; Tian, Z.; Yuan, S., *J. Mag. Mag. Mater.* 2019, 469, 504-509; <https://doi.org/10.1016/j.jmmm.2018.09.026>
- [31] Chakraverty, S.; Ghosh, B.; Kumar, S.; Frydman, A., *Appl. Phys. Lett.* 2006, 88, 042501; <https://doi.org/10.1063/1.2166203>

- [32] Tsoi, G.M.; Senaratne, U.; Tackett, R.J.; Buc, E.C.; Naik, R., *J. Appl. Phys.* 2005, 97, 10J507; <https://doi.org/10.1063/1.1853898>
- [33] Tian, Z.; Xu, L.; Gao, Y.; Yuan, S.; Xia, Z., Magnetic memory effect at room temperature in exchange coupled NiF
- [34] Dhara, S.; Chowdhury, R.R.; Bandyopadhyay, B., *RSC Adv.* 2015, 5, 95695-95702' <https://doi.org/10.1039/C5RA19178E>
- [35] T. Dietl, H. Ohno, F. Matsukura, J. Cibertand, D. Ferrand, *Science* 2871019(2000).
- [36] J. Wu, C.-W. Nan, Y. Lin, Y. Deng, *Phys. Rev. Lett.* 89217601 (2002).
- [37] O. Bidault, M. Maglione, M. Actisand, M. Kchikech, *Phys. Rev. B* 524191(1995).
- [38] J. Wang, J. Cai, Y.-H. Linand, C.-W. Nan, *Appl. Phys. Lett.* 87, 202501 (2005); <https://doi.org/10.1063/1.2130532>
- [39] R. H. Kodama, S. A. Makhlofand, A. E. Berkowitz, *Phys. Rev. Lett.* 791393 (1997)
- [40] J. Nowotnyand, M. Rekas, *Solid State Ionics* 12253(1984).
- [41] M. Subash, M. Chandrasekar, S. Panimalar, C. Inmozhi, R. Uthrakumar, *Materials Today Proceedings*.
- [42] Chigane M., Isikawa M. (1994), *J. Electrochem. Soc.* 1413439.